

# Mechanical Characteristics of Superplastic Deformation of AZ31 Magnesium Alloy

Fadi K. Abu-Farha and Marwan K. Khraisheh

(Submitted April 20, 2006; in revised form October 22, 2006)

As the lightest constructional metal on earth, magnesium (and its alloys) offers a great potential for weight reduction in the transportation industry. Many automotive components have been already produced from different magnesium alloys, but they are mainly cast components. Production of magnesium outer body components is still hindered by the material's inferior ductility at room temperature. Magnesium alloys are usually warm-formed to overcome this problem; however, it was observed that some magnesium alloys exhibit superior ductility and superplastic behavior at higher temperatures. More comprehensive investigation of magnesium's high temperature behavior is needed for broader utilization of the metal and its alloys. In this work, the high temperature deformation aspects of the AZ31B-H24 commercial magnesium alloy are investigated through a set of uniaxial tensile tests that cover forming temperatures ranging between 23 and 500 °C, and constant true strain rates between  $2 \times 10^{-5}$  and  $2.5 \times 10^{-2} \text{ s}^{-1}$ . The study targets mainly the superplastic behavior of the alloy, by characterizing flow stress, elongation-to-fracture, and strain rate sensitivity under various conditions. In addition, the initial anisotropy is also investigated at different forming temperatures. The results of these and other mechanical and microstructural tests will be used to develop a microstructure-based constitutive model that can capture the superplastic behavior of the material.

**Keywords** AZ31magnesium alloy, formability, high temperature deformation, initial anisotropy, strain rate sensitivity, superplasticity

## 1. Introduction

Along with the enormous developments, the automotive industry has been achieving recently; the demand for lower fuel consumption vehicles has been growing side by side, mainly due to environmental and economical issues. The automotive industry has been under pressure that led to the commitment in 1990 to reduce fuel consumptions by 25% in 15 years (Ref 1).

Proposed ways to reduce fuel consumption and exhaust emissions include aerodynamics, alternative fuels and mass reduction. Among all, reduction of mass is the most influential and least costly, if large reductions of 20–40% are to be achieved (Ref 2). Daimler-Benz, VW and Audi AG have shown in separate studies that more than 50% of fuel consumption is mass dependent (Ref 1, 3, 4). Audi concluded that a 6% drop in fuel consumption can be achieved by a 10% mass drop (Ref 1).

This article was presented at the AeroMat Conference, International Symposium on Superplasticity and Superplastic Forming (SPF) held in Seattle, WA, June 6–9, 2005.

Fadi K. Abu-Farha, and Marwan K. Khraisheh, Center for Manufacturing and Department of Mechanical Engineering, University of Kentucky, Lexington, KY 40506. Contact e-mail: Khraisheh@engr.uky.edu.

On the other hand, growing customer demand for enhanced comfort and safety measures caused the weight of cars to increase continuously, making the achievement of lighter cars more difficult and challenging (Ref 3, 5).

Therefore and in order to satisfy all these growing demands and achieve a significant weight reduction, the automotive industry had to reformulate the concept of light weight structures both in terms of mechanical design and lightweight materials.

Magnesium is the lightest constructional metal on earth; the  $1.74 \text{ g/cm}^3$  density makes magnesium 35% lighter than aluminum ( $2.70 \text{ g/cm}^3$ ), and 78% lighter than steel ( $7.85 \text{ g/cm}^3$ ) (Ref 6). This attractive attribute has put magnesium into the production lines of VW since the end of WWII, where air-cooled engines and gearboxes were made of AZ81 & AS41 magnesium alloys (Ref 4). The first age of magnesium, as described by Friedrich et al. (Ref 7), reached its peak in 1971. However, cheaper prices and technical superiority of aluminum alloys diminished the importance of magnesium as a material by the early 80s.

Shortly afterwards, the interest in magnesium and its alloys was revived, as the metal offers a great potential for weight reduction by replacing steel and aluminum, if proper design considerations are made. This has been embodied by the continuously growing research efforts in various related fields, and the increasing number of automotive components that have been successfully produced from different magnesium alloys (Ref 3, 4, 7). Despite the remarkable advancements, most of the successfully produced magnesium auto parts are cast-components. Significant weight reduction cannot be achieved unless magnesium usage is expanded to cover other areas, mainly sheet metal outer body panels. The metal's inferior ductility at room temperature still hinders such an expansion.

Magnesium wrought alloy AZ31 is commercially available in sheet form, and offers very good mechanical properties. Matching stiffness ( $E$ ) and strength ( $\sigma_{YS}$  or  $\sigma_{TS}$ ) requirements, AZ31 promises a significant mass reduction in large surface area/thin walled applications (About 20% reduction compared to aluminum, and 50% compared to steel). Yet, inherited by the metal's HCP crystal structure, very limited ductility accompanied by brittle-like behavior can be achieved at room temperature. To acquire a behavior (formability) similar to that of steel or aluminum at room temperature, AZ31 has to be warm-formed at about 225 °C (437 F). Indeed, warm forming has been a good relief for this problem, enabling successful forming of some automotive components, mainly by deep drawing (Ref 8–11).

Surprisingly, AZ31's room temperature inferior ductility turns into large uniform ductility under certain higher temperature conditions; the alloy is shown to exhibit superplastic nature under those conditions (Ref 12–15). Superplasticity; is the phenomenon of extraordinary tensile ductility exhibited by a certain class of fine-grained metals when deformed under controlled rates, at relatively high temperatures. Many titanium and aluminum alloys are successfully formed to produce aerospace and automotive components, by means of the Superplastic Forming Technique (SPF).

For magnesium in general, and the AZ31 in particular, SPF offers a solution for the metal's room temperature poor ductility and deformation's non-uniformity. If the process is optimized, AZ31 sheets can be successfully superplastically formed, promising a lower-cost production and remarkable weight-saving potential.

Recently, a large number of studies investigated the formability and deformation aspects of the AZ31 Mg alloy at various temperatures. The different researchers targeted different aspects in their respective studies, including warm formability, high temperature deformation, and superplasticity, cavitation and microstructural evolution, and anisotropy.

Doege et al. (Ref 8, 9, 11), Droeder et al. (Ref 10) and Siegert et al. (Ref 16) have done significant amount of work on the warm forming of AZ31 alloy, under uniaxial and biaxial loading conditions. Uniaxial tensile tests, deep drawing and gas bulge forming were carried out at various strain rates, covering temperatures up to 250 °C. Their practices proved that AZ31 is warm-formable, producing some components for potential automotive applications.

Many other investigators studied the behavior of the alloy at higher temperatures, highlighting the effect of various parameters, mainly temperature, strain rate, and texture, on the enhanced ductility of the alloy (Ref 14, 15, 17–20).

Superplastic behavior in the AZ31 alloy was observed in many studies, and was given special attention by a number of researchers. However, the majority of those studies covered limited forming temperatures (Ref 12, 13, 21–25) and/or strain rates (Ref 13, 21, 26). Lee et al. (Ref 18) covered in their tests temperatures between 250 and 500 °C over a wide range of strain rates,  $10^{-4}$ – $100 \text{ s}^{-1}$ . Their experiments aimed at studying the deformation mechanisms and establishing the processing map of the alloy, and their published data does not cover the response of the material in terms of flow stress, fracture strain, and strain rate sensitivity.

There is no single comprehensive study that covers all the mechanical aspects of deformation of AZ31 Mg alloy (flow stress, elongation-to-fracture, and strain rate sensitivity) over a wide range of temperatures and strain rates. In addition, it is

difficult to compile the results of the different researchers who covered various aspects of the alloy's deformation due to variation in testing procedures, loading paths, and the initial microstructure of the alloy (Ref 21, 24, 25, 27–29).

Microstructural evolution in terms of grain growth and cavitation has also been studied, due to its strong influence on the limiting fracture strain, and the post forming attributes of the alloy (Ref 23, 28–30). Wu et al. (Ref 30) investigated the static grain growth in the AZ31 at elevated temperatures up to 500 °C, but did not model or show the variations of grain size over the different temperatures. Lee et al. (Ref 29) on the other hand showed the effects of time, temperature and strain rate on the grain growth of AZ31, but for limited temperatures and strain rates. Similarly, cavitation studies (Ref 23, 28, 29) covered limited temperatures and strain rates.

Kaiser et al. (Ref 31, 32) was one of few to highlight the issue of initial anisotropy exhibited by the AZ31 alloy, both at room temperature and temperatures up to 250 °C. No comprehensive data has been published on the initial state of anisotropy, and more importantly, the deformation-induced anisotropy in the AZ31 at elevated temperatures.

Despite the large number of studies available, there is still a need for more tests in order to develop a comprehensive database for AZ31 deformation. The database is essential to develop accurate multiaxial microstructure-based constitutive model that can be used to optimize the SPF of Mg AZ31 and advance the industrial use of AZ31 on a larger scale. The model must account for possible changes in the microstructure and anisotropy during deformation.

This work presents an experimental study on the various deformation characteristics of the AZ31 magnesium alloy over a wide range of temperatures and strain rates. Constant strain rate uniaxial tensile tests were conducted within a forming temperature range of 23–500°C, where the strain rate is varied between  $2 \times 10^{-5}$  and  $2.5 \times 10^{-2} \text{ s}^{-1}$ . Tensile test specimens were cut at 0°, 45°, and 90° with respect to the rolling direction of the as received sheet. The effects of temperature and strain rate on the behavior of the material are emphasized, and the region in which the material exhibits superplastic behavior is highlighted for further testing. Initial implications of superplasticity were mainly large ductility (>200%) and high strain rate sensitivity ( $m > 0.3$ ). The strain sensitivity index was measured from the constructed stress/strain rate sigmoidal-shaped curves and also using strain rate jump tests in the designated superplastic region. The results of the two methods are also discussed.

Initial anisotropy was also examined in this work. The 45° and 90° samples were tested at selected temperatures and various strain rates, and the results were compared to the ones corresponding to the 0° samples. Room temperature tests were essential to characterize the initial state of anisotropy in the as received material, while high temperature tests aimed at studying the influence of temperature on anisotropy.

## 2. Testing Equipment and Experimental Procedure

The equipment used to conduct the tensile tests throughout this study is the INSTRON 5582 universal testing machine, equipped with electrical resistance heating chamber (furnace) that provides a maximum temperature of 610 °C, and can

maintain a temperature variation of  $\pm 1$  °C. The machine is equipped with a  $\pm 100$  KN load cell, which was often replaced by a  $\pm 5$  KN load cell for more refined load measurements during the high temperature tests. The material used throughout this study is the commercial alloy AZ31B-H24 in the form of 3.22 mm (0.125 in.) thick sheet, with an average initial grain size of about 5  $\mu\text{m}$ . The dimension of the gauge section of the test sample is 19  $\times$  6 mm. Samples were cut from the sheet at different directions (0°, 45°, and 90°) with respect to the rolling direction.

Special grips were used to secure the test sample inside the heating chamber, and the 'specimen protect' controller is activated before the heating phase is started. This controller induces the cross-head beam to move up or down in a way that maintains a very small preset load value ( $\pm 2.5$  N), allowing the test sample and the grips to expand without distorting the sample. When the desired temperature is reached, some additional equilibrium time is allowed, after which the test is started. Stress measurement is directly obtained from the load cell reading and strain measurement is established from the direct displacement of the cross-head beam. More details about the grips, heating time, testing procedure and discussions about the effects of various testing conditions on the accuracy of the results are discussed in an accompanying paper (Ref 33).

### 3. Uniaxial Tensile Tests and Mechanical Properties

The 0° samples were the first to be tested under uniaxial simple tension, where the tests were classified into three groups based on the forming temperature:

- From previous tests (Ref 15), temperatures higher than 300 °C are needed to achieve wide-range superplasticity in the alloy. So, high temperature tests were conducted between 325 and 500 °C, in a 25 °C increment.
- 225 °C was chosen as a warm forming temperature (Ref 8, 16) and aimed to be a reference for evaluating the enhancement of ductility achieved by superplasticity.
- Room temperature tests at 23 °C were mainly aimed to evaluate the initial state of anisotropy of the material.

For each forming temperature, a group of constant strain rate tests were conducted between  $2 \times 10^{-5}$  and  $1 \times 10^{-2}$  s<sup>-1</sup>. Two main attributes were extracted from each of these tests, flow stress and fracture strain.

#### 3.1 Effect of Strain Rate on Stress/Strain Curves

Two groups of true stress/strain curves corresponding to 375 °C and 400 °C forming temperatures are shown in Fig. 1 for different strain rates. Strong flow stress sensitivity to strain rate is depicted from both groups; the higher the strain rate, the higher the flow stress of the material. On the other hand, the maximum attainable elongation is inversely proportional to the imposed strain rate.

Stress/strain curves do not clearly reflect how uniform the deformation is, yet, a measure for comparison can be made based on the hardening/softening behavior. Considering the two sets of curves, it is observed that the material exhibits strain softening at high strain rates, which diminishes gradually and

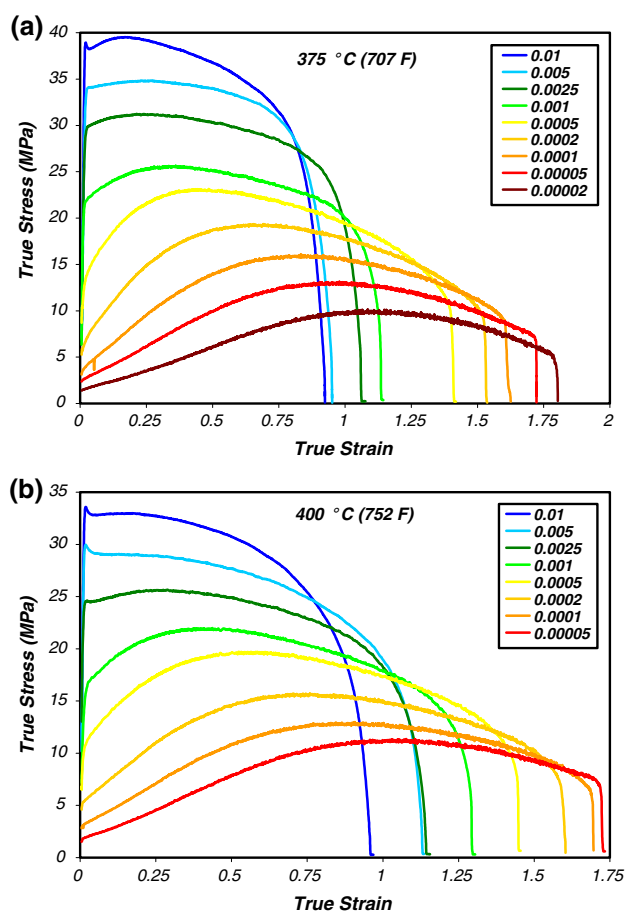


Fig. 1 Effect of strain rate on the stress/strain curves at (a) 375 °C (b) 400 °C



Fig. 2 Deformed samples under various strain rates at 400 °C

turns into strain hardening as the strain rate decreases. It is generally true that stronger softening reflects more non-uniform deformation; for that, uniformity of deformation can be enhanced at higher temperatures by reducing the strain rate.

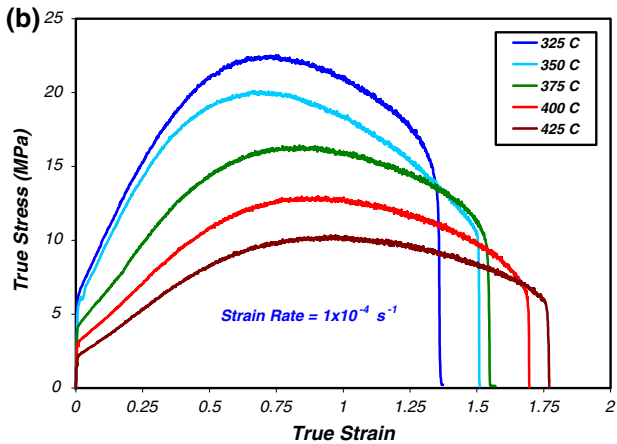
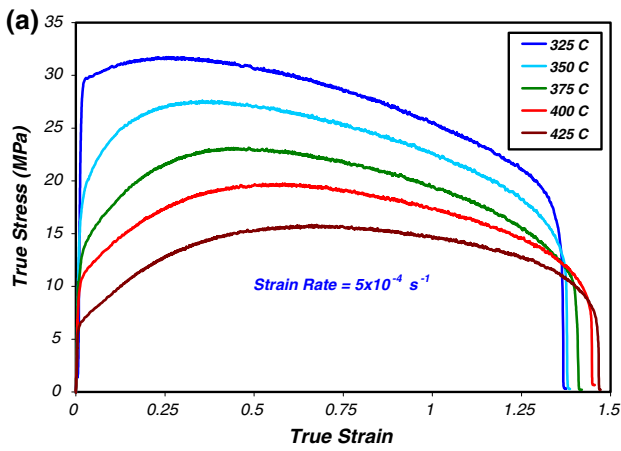


Fig. 3 Effect of temperature on the stress/strain curves at (a)  $5 \times 10^{-4} \text{ s}^{-1}$  (b)  $1 \times 10^{-4} \text{ s}^{-1}$

This is clearly shown in Fig. 2, which shows the deformed samples at 400 °C.

### 3.2 Effect of Temperature on Stress/Strain Curves

By fixing the strain rate and varying the temperature, similar behavior is observed. Figure 3 shows two similar groups of true stress/strain curves corresponding to  $5 \times 10^{-4}$  and  $1 \times 10^{-4} \text{ s}^{-1}$  strain rates at different temperatures. Generally speaking, raising the temperature enhances ductility, in terms of both uniformity and the maximum attainable strain. In some cases, however, increasing the temperature beyond a certain point can adversely affect the tensile ductility of the alloy.

### 3.3 Stress/Strain Rate Curves

The logarithmic stress/strain rate curves for five different temperatures are shown in Fig. 4. The sigmoidal-shaped curves are typical for superplastic deformation. The strain rate sensitivity of the material at any combination of temperature and strain rate is reflected by the index  $m$ , represented by the slope of each curve at a given point. The profiles of  $m$  at different temperatures were estimated using these curves, as shown in Fig. 5.

As depicted from Fig. 4,  $m$  is expected to be maximum in the neighborhood of  $2 \times 10^{-4} \text{ s}^{-1}$ , at about 375–400 °C.

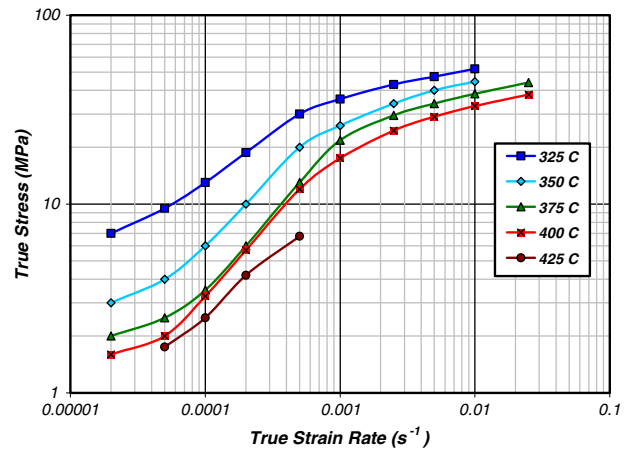


Fig. 4 Stress/strain rate sigmoidal-shaped curves at various temperatures

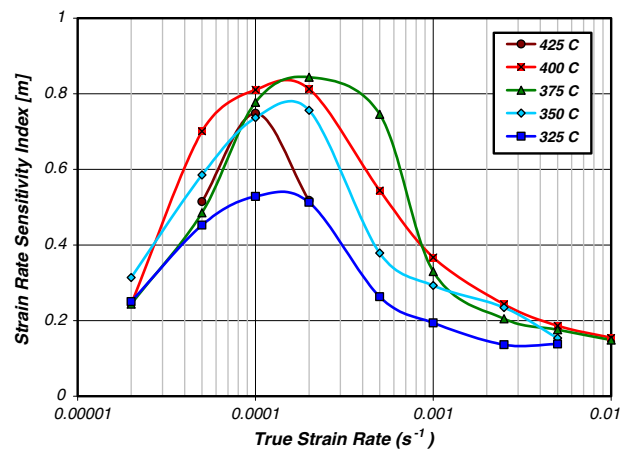


Fig. 5 Strain rate sensitivity index  $m$  for various temperatures, from the stress/strain rate curves

Investigation of the test samples deformed at the different temperatures and strain rates indicated the highest degrees of deformation uniformity in the aforementioned region.

Figure 5, on the other hand, supports this; but one can easily notice the high values of  $m$  (up to 0.83), which do not seem to be realistic! To tackle this problem, accurate quantitative evaluation of  $m$  was made through a series of strain rate jump tests, which are discussed in the second set of tests.

### 3.4 Ductility

Two general guidelines for enhancing the tensile ductility during high temperature tests were drawn earlier in the discussion; higher temperature and lower strain rate. Figure 6 schematically explains this through the results of the uniaxial tensile tests, and shows the effect of each of the two parameters independently.

For the considered range of temperatures and strain rates, and beyond which forming process might be impractical ( $>450 \text{ °C}$  and  $<1 \times 10^{-4} \text{ s}^{-1}$ ), the two sets of curves lead to some interesting observations, mainly:

- For a fixed temperature, decreasing the strain rate produces a more observable ductility-enhancement compared

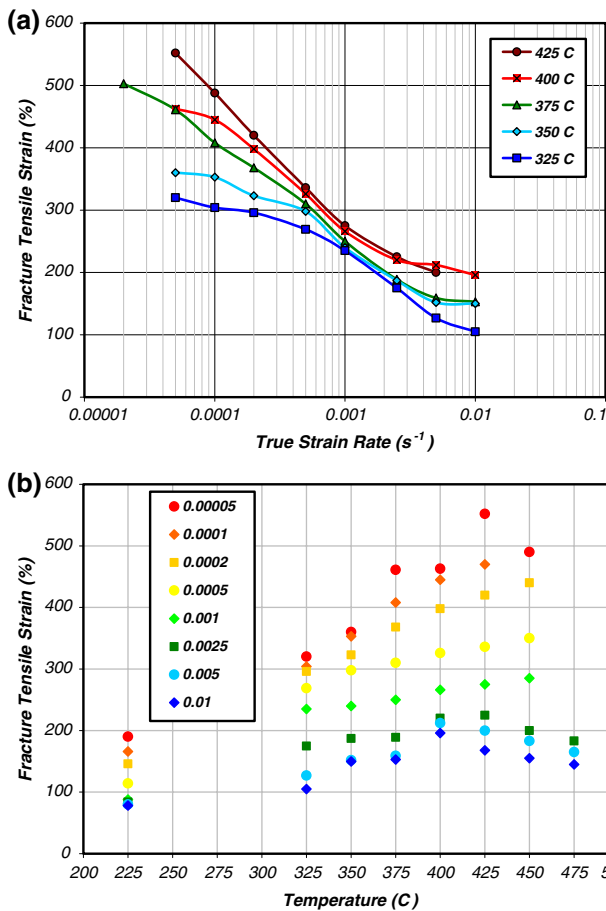


Fig. 6 Fracture uniaxial tensile strain versus (a) strain rate (b) temperature

to the case when the strain rate is held fixed and the temperature is raised.

- Since a 200% elongation can be considered as an initial indicative of superplasticity, it can be inferred that about  $10^{-3} \text{ s}^{-1}$  strain rate is the threshold for superplasticity for all the considered high temperature tests ( $>325 \text{ }^\circ\text{C}$ ).
- Figure 6(b) includes the results of the tests conducted at  $225 \text{ }^\circ\text{C}$  (warm forming), from which it is observed that a 200% elongation is not feasible, even at the smallest strain rates considered.
- As indicated before, Fig. 6(b) clearly shows that for each strain rate, there is a limiting temperature beyond which no further ductility-enhancement can be achieved. In fact, the maximum attainable elongation declines afterwards.

The other concern related to ductility, is the uniformity of deformation. It is of high importance in the actual forming of any component to achieve a certain level of deformation-uniformity, to avoid any severe localized necking that leads to premature failure. Test results indicated that uniformity of deformation goes along with ductility enhancement, to a very high extent. In general, more uniform deformation is usually associated with higher elongation-to-fracture. This is also illustrated in Fig. 2, which shows the deformed samples at  $400 \text{ }^\circ\text{C}$ . However, deformation-uniformity deviates from this conclusion at very low strain rates due to the escalation of void growth.

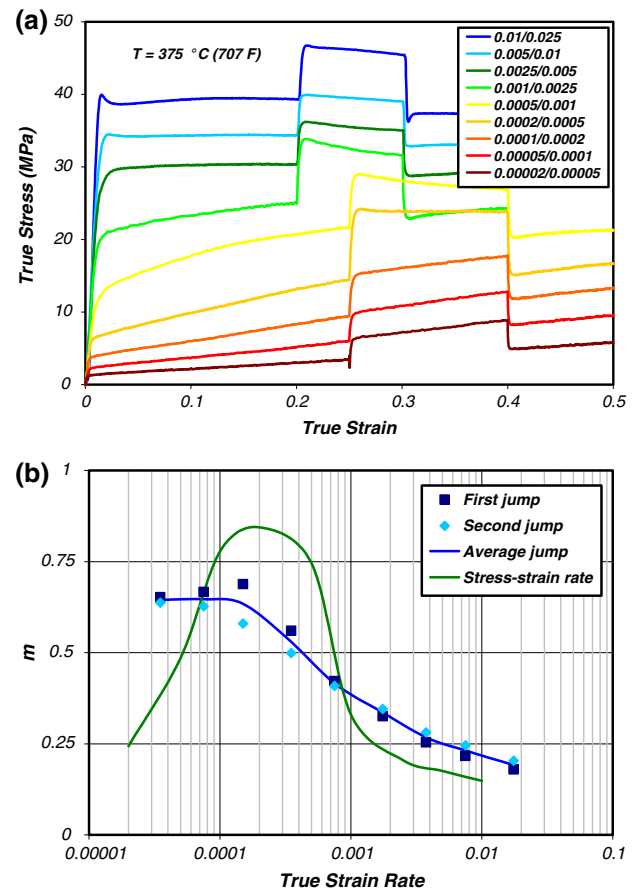


Fig. 7 (a) Strain rate jump tests at  $375 \text{ }^\circ\text{C}$  (b) Strain rate sensitivity index  $m$  [Strain rate jump tests versus the stress/strain rate curve]

#### 4. Strain Rate Jump Tests

Strain rate jump tests were conducted at  $375 \text{ }^\circ\text{C}$ . The jump was imposed between 0.2 and 0.3 strains, for the high strain rate tests, and between 0.25 and 0.4 strains, for the low strain rate tests. All the stress/strain curves are shown in Fig. 7(a).

For each curve, two values of  $m$  were evaluated;  $m_1$  from the first (upward) jump, and  $m_2$  from the second (downward) jump.  $m_1$  and  $m_2$ , in addition to their average are all plotted in Fig. 7(b). Slight differences between  $m_1$  and  $m_2$  were observed, since the value of  $m$  depends on the strain at which it is estimated. But more significant deviation was observed when the curve obtained from the flow stress/strain rate curve was compared to them.

Estimating  $m$  using the flow stress/strain rate curve reflects the strain rate sensitivity of the material in the very early stages of deformation, because the flow stress is determined at low strain values. While in a strain rate jump test,  $m$  is evaluated at some other strain value. Add to this, the point on the stress/strain curve at which the value of flow stress is taken might be unclear in some cases. And since the stress/strain rate curve cannot be guaranteed smooth, the different segments of the curve will reflect either higher or lower values for  $m$ , as it is the case here.

Strain rate jump test is believed to be the more accurate way for evaluating  $m$ . Currently, tests are being carried out with

multi-jumps at different strains, to understand the effect of strain on the value of  $m$ .

## 5. Initial Anisotropy

### 5.1 Room Temperature Anisotropy

Tensile tests at room temperature were carried out over a number of strain rates, using samples cut at three different orientations with respect to the rolling direction,  $0^\circ$ ,  $45^\circ$ , and  $90^\circ$ . Figure 8 shows the stress/strain curves corresponding to each

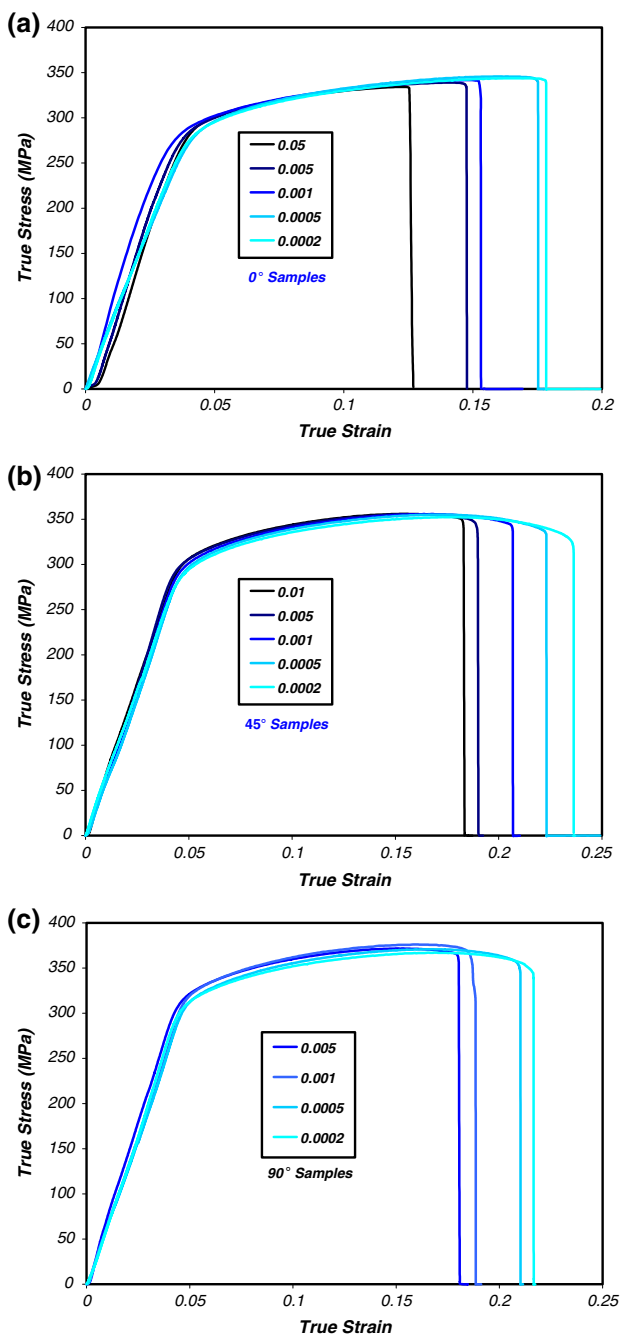


**Fig. 8** Stress/strain curves at different strain rates for samples cut at (a)  $0^\circ$  (b)  $45^\circ$  (c)  $90^\circ$  to the rolling direction

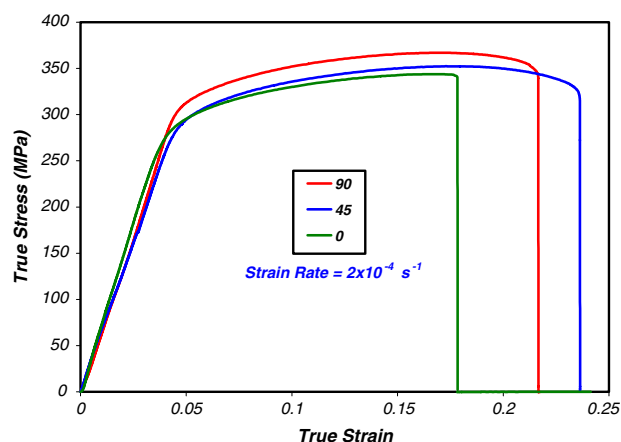


**Fig. 9** Room-temperature anisotropy at  $2 \times 10^{-4} \text{ s}^{-1}$  for samples cut at  $0^\circ$ ,  $45^\circ$ , and  $90^\circ$  with respect to the rolling direction

family of samples. It is observed that for each set of curves, the flow stress (yield stress in this case) is strain rate insensitive. Small influence on the tensile ductility is observed. Lowering the imposed strain rate enhances the ultimate tensile elongation, with a negligible effect on the yield strength of the material.

By comparing the three sets of curves, it is noticed that the  $0^\circ$  samples exhibits the lowest tensile ductility at any strain rate. This can be clearly depicted from Fig. 9, which shows the stress/strain curves for the three differently-oriented samples at  $2 \times 10^{-4} \text{ s}^{-1}$ . The  $45^\circ$  sample exhibits a slightly higher elongation-to-fracture compared to the  $90^\circ$  one, but both clearly exceed that exhibited by the  $0^\circ$  sample. On the other hand, the yield stresses are not quite the same;  $\sigma_{Y,90^\circ} > \sigma_{Y,45^\circ} > \sigma_{Y,0^\circ}$ . These observations can be generalized to the other strain rates as illustrated in Fig. 8.

Kaiser et al. (Ref 31) conducted a more detailed investigation, by considering samples cut at various orientations with respect to the rolling direction, ranging between  $0^\circ$  and  $90^\circ$ , with a  $10^\circ$  increment. A plot for yield strength as a function of sample's angle of cut clearly shows a direct proportionality, which supports our conclusion here. In addition, in a plot for elongation-to-fracture versus the angle of cut, similar behavior as the one observed here is noticed, but with smaller differences. One of the reasons might be that Kaiser et al. considered only one strain rate value in the aforementioned tests.

### 5.2 High Temperature Anisotropy

Two temperatures,  $375$  and  $400^\circ\text{C}$ , and a strain rate of  $2 \times 10^{-4} \text{ s}^{-1}$ , were selected for a preliminary investigation of the effect of the orientation of the test sample on the mechanical properties during high temperature testing of AZ31. The stress/strain curves for the three samples are shown in Fig. 10.

For each of the two considered temperatures, small differences between the curves corresponding to the three samples are observed, in terms of flow stresses in particular. The effect on the maximum elongation might be more observable; but yet, the differences are not strong enough to draw a conclusion in this regard.

However, it can be said that the initial anisotropy is less significant at higher temperatures. This result is in agreement with Kaiser et al. (Ref 31) who examined the effect of temperature on initial anisotropy and observed that anisotropy

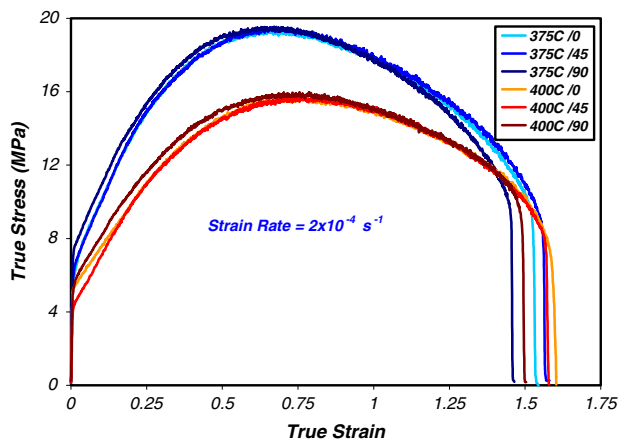


**Fig. 10** High-temperature anisotropy at  $2 \times 10^{-4} \text{ s}^{-1}$  for samples cut at  $0^\circ$ ,  $45^\circ$ , and  $90^\circ$  with respect to the rolling direction

decreases constantly with rising temperature, to become almost unobservable at  $250^\circ \text{C}$ .

Anisotropy is one of the highly-influential, yet seldom-covered, parameters in high temperature testing. It is important to note that the uniaxial tensile tests can only provide information on the initial state of anisotropy and can not provide information on possible deformation-induced anisotropy. Other tests that involve multiaxial loading are required for better characterization of the anisotropic behavior of the material (Ref 34, 35).

## 6. Conclusions

This work presents a study on the high temperature deformation aspects of the AZ31 magnesium alloy, through a set of uniaxial tensile tests. The study covered temperatures between  $23$  and  $500^\circ \text{C}$ , over a wide range of strain rates. Tests at temperatures higher than  $325^\circ \text{C}$  aimed at characterizing the superplastic behavior of the alloy in terms of flow stress, elongation-to-fracture, and strain rate sensitivity. Strain rate jump tests were shown to be the more accurate and reliable way for evaluating the strain rate sensitivity  $m$ . The initial state of anisotropy was investigated and found to be more significant at room temperature than at elevated temperatures. These comprehensive mechanical results will be combined with microstructural results, currently being analyzed, to develop and calibrate a multiaxial microstructure-based constitutive model. The model is based on the theory of viscoplasticity and has a microstructure-based overstress function.

## Acknowledgment

The support of the National Science Foundation, CAREER Award # DMI-0238712, is acknowledged.

## References

1. D. Engelhart and C. Moedel, Die Entwicklung des Audi A2, ein neues Fahrzeugkonzept in der Kompakwagenklassen (The Development of the Audi A2, a New Vehicle Concept in the Compact Car Class), Technologien um das 31-Auto, November 16–18, 1999 (Brunswick, Germany), p 11–21, in German

2. G. Cole, How Magnesium Can Achieve High Volume Usage in Ground Transportation, Magnesium into the Next Millennium, The 56th Annual Meeting of the International Magnesium Association, June 6–9, 1999 (Rome, Italy), p 21–30
3. A. Jambor and M. Beyer, New Cars - New Materials, *Mater. Des.*, 1997, **18**(4-6), p 203–209
4. S. Schumann and F. Friedrich, The Use of Magnesium in Cars - Today and in the Future, Mg Alloys and their Applications, April 28–30, 1998 (Wolfsburg, Germany)
5. D. Carle and G. Blount, The Suitability of Aluminum as an Alternative Material for Car Bodies, *Mater. Des.*, 1999, **20**(5), p 267–272
6. Tabellenbuch Metall, 41st ed., 6th pr., Verlag Europa Lehrmittel, 2001, in German
7. H. Friedrich and S. Schumann, The Second Age of Magnesium: Research Strategies to Bring the Automotive Industry's Vision to Reality, The Second Israeli International Conference on Mg Science and Technology, February 2000 (Sdom, Israel), p 9–18
8. E. Doege and K. Dröder, Sheet Metal Forming of Magnesium Wrought Alloys – Formability and Process Technology, *J. Mater. Process. Technol.*, 2001, **115**, p 14–19
9. E. Doege, L-E. Elend, and F. Meiners, Comparative Study of Massive and Sheet Lightweight Components Formed of Different Lightweight Alloys for Automotive Applications, ISATA 33rd 2000: Automotive & Transportation Technology, September 25–27, 2000 (Dublin, Ireland), p 87–94
10. K. Dröder and St. Janssen, Forming of Magnesium Alloys – A Solution for Lightweight Construction, 1999 International Body Engineering Conference Proceedings, SAE, 1999 (Detroit, Michigan)
11. E. Doege, W. Sebastian, K. Dröder, and G. Kurz, Increased Formability of Mg-Sheets Using Temperature Controlled Deep Drawing Tools, Proceedings of the Second Global Symposium on Innovations in processing and Manufacturing of Sheet Materials, TMS 2001, p 53–60
12. H. Watanabe, H. Tsutsui, T. Mukai, Y. Okanda, M. Kohzu, and K. Higashi, Superplastic Behavior in Commercial Wrought Magnesium Alloys, *Mater. Sci. Forum*, 2000, **350–351**, p 171–176
13. W. Kim, S. Chung, C. Chung, and D. Kum, Superplasticity in Thin Magnesium Alloy Sheets and Deformation Mechanism Maps for Magnesium Alloys at Elevated Temperatures, *Acta Mater.*, 2001, **49**(16), p 3337–3345
14. L. Tsao, C. Wu, and T. Chuang, Evaluation of Superplastic Formability of the AZ31 magnesium Alloy, *Mater. Res. Adv. Tech.*, 2001, **92**(6), p 572–577
15. F. Abu-Farha and M. Khraisheh, Deformation Characteristics of AZ31 Magnesium Alloy Under Various Forming Temperatures and Strain Rates, Proceedings of the 8th ESAFORM Conference on Material Forming, April 27–29, 2005 (Cluj-Napoca, Romania), p 627–630
16. K. Siegert, S. Jäger, and M. Vulcan, Pneumatic Bulging of Magnesium AZ31 Sheet Metals at Elevated Temperatures, *Ann. CIRP*, 2003, **52**, p 241–244
17. A. Jäger, P. Lukas, V. Gärtnerova, J. Bohlen, and K. Kainer, Tensile Properties of Hot Rolled AZ31 Mg Alloy Sheets at Elevated Temperatures, *J. Alloy. Compd.*, 2004, **378**, p 184–187
18. B. Lee, K. Shin, and C. Lee, High Temperature Deformation Behavior of AZ31 Mg Alloy, *Mater. Sci. Forum*, 2005, **475–479**, p 2927–2930
19. S. Agnew and O. Duygulu, A Mechanistic Understanding of the Formability of Magnesium: Examining the Role of Temperature on the Deformation Mechanisms, *Mater. Sci. Forum*, 2003, **419–422**, p 177–188
20. H. Watanabe, A. Takara, H. Somekawa, T. Mukai, and K. Higashi, Effect of Texture on Tensile Properties at Elevated Temperatures in an AZ31 Magnesium Alloy, *Scr. Mater.*, 2005, **52**, p 449–454
21. J. Tan and M. Tan, Superplasticity in a Rolled Mg-3Al-1Zn Alloy by Two-Stage Deformation Method, *Scr. Mater.*, 2002, **47**(2), p 101–106
22. M. Mabuchi, M. Nakamura, T. Asahina, H. Iwasaki, T. Aizawa, and K. Higashi, Microstructural Evolution and Superplasticity of Rolled Mg-9Al-1Zn, *Mater. Sci. Eng. A*, 2000, **290**(1–2), p 139–144
23. Y. Chino and H. Iwasaki, Cavity Growth Rate in Superplastic 5083 Al and AZ31 Mg Alloys, *J. Mater. Res.*, 2004, **19**(11), p 3382–3388
24. A. Ben-Artzy, A. Shtechman, A. Bussiba, Y. Salah, S. Ifergan, M. Kupiec, and R. Grinfeld, Low Temperature Super-plasticity Response of AZ31B Magnesium Alloy with Severe Plastic Deformation, Magnesium Technology 2003, Proceedings of the 2003 TMS Annual Meeting, 2003 (San Diego, California), p 259–263

25. A. Bussiba, A. Ben Artzy, A. Shtechman, S. Ifergan, and M. Kupiec, Grain Refinement of AZ31 and AZ60 Mg Alloys – Towards Superplasticity Studies, *Mater. Sci. Eng. A*, 2001, **302**(1), p 56–62
26. X. Wu and Y. Liu, Superplasticity of Coarse-Grained Magnesium Alloy, *Scr. Mater.*, 2002, **46**(4), p 269–274
27. D. Yin, K. Zhang, G. Wang, and W. Han, Superplasticity of Fine-Grained AZ31 Mg Alloy Sheets, *T. Nonferr. Metal. Soc.*, 2004, **14**(6), p 1100–1105
28. D. Yin, K. Zhang, G. Wang, and W. Han, Superplasticity and Cavitation in AZ31 Mg Alloy at Elevated Temperatures, *Mater. Lett.*, 2005, **59**, p 1714–1718
29. C. Lee and J. Huang, Cavitation Characteristics in AZ31 Mg Alloys During LTSP or HSRSP, *Acta Mater.*, 2004, **52**, p 3111–3122
30. X. Wu, Y. Liu, and H. Hao, High Strain Rate Superplasticity and Microstructure Study of a Magnesium Alloy, *Mater. Sci. Forum*, 2001, **357–359**, p 363–370
31. F. Kaiser, D. Letzig, J. Bohlen, A. Styczynski, C. Hartig, and K. Kainer, Anisotropic Properties of Magnesium Sheet AZ31, *Mater. Sci. Forum*, 2003, **419–422**, p 315–320
32. F. Kaiser, J. Bohlen, D. Letzig, K. Kainer, A. Styczynski, and C. Hartig, Influence of Rolling Conditions on the Microstructure and Mechanical Properties of Magnesium Sheet AZ31, *Adv. Eng. Mater.*, 2003, **5**(12), p 891–896
33. F. Abu-Farha and M. Khraisheh, On the High Temperature Testing of Superplastic Materials. ASM Journal of Materials Engineering and Performance, Doi: 10.1007/s11665-007-9024-4
34. M. Khraisheh, H. Zbib, C. Hamilton, and A. Bayoumi, Constitutive Modeling of Superplastic Deformation. Part I: Theory and Experiments, *Int. J. Plasticity*, 1997, **13**(1–2), p 143–164
35. F. Abu-Farha and M. Khraisheh, Constitutive Modeling of Deformation-Induced Anisotropy in Superplastic Materials, *Mater. Sci. Forum*, 2004, **447–448**, p 165–170